61

INITIAL STAGES OF ANODIC OXIDATION OF POLYCRYSTALLINE COPPER ELECTRODES IN ALKALINE SOLUTION

JOHN M.M. DROOG, CORRIE A. ALDERLIESTEN, PETER T. ALDERLIESTEN and
GOSSE A. BOOTSMA

Van't Hoff Laboratory, State University of Utrecht, Padualaan 8, Utrecht (The Netherlands)

ABSTRACT

   The first stages of the anodic oxidation of polycrystalline copper electrodes in NaOH
solutions were studied by potential sweep voltammetry and ellipsometry. Formation of bulk
Cu_2O was found to be preceded by electrosorption of oxygen species, that occurs in two
successive stages, each represented by a current peak, corresponding to a different submono-
layer state with a different adsorption energy. This surface oxide was formed via random
electrodeposition. The width of the first current peak indicates the presence of lateral attrac-
tive interactions in the chemisorbed layer. The surface layer did not show any ageing effect.

(I) INTRODUCTION

Although the anodic oxidation of copper in alkaline solutions has been exten-
sively studied by means of galvanostatic [1—7] and potentiodynamic tech-
niques [7—20], the initial oxidation processes have received little attention. A
study of the first oxidation processes on the bare metal surface should help us
to obtain a better understanding of the copper anode.
   Ambrose et al. [11] reported cyclic voltammograms of copper in 1 mol
dm^{-3} KOH. A voltammogram similar to the one they published is shown in
Fig. 1, for copper in 1 mol dm^{-3} NaOH. They were the first to observe by
careful examination at high sensitivity, and especially at higher sweep rates, the
presence of a very small peak (peak 1 in Fig. 1) with a potential negative to the
peak due to formation of Cu_2O (peak 2). Peak 3 is generally associated with
formation of Cu(II) species [11,13,19,20]. Peaks 4 and 5 correspond to the
Cu(II)/Cu(III) redox couple [11,19]. Peak 6 is assigned to reduction of Cu(II)
to Cu(I) [11,13] or to reduction of Cu(I) to Cu [19], and peak 7 represents
complex electroreduction to Cu [11,13,19].
   Peak 1 was tentatively assigned by Ambrose et al. to the formation of
soluble species according to

$$Cu + 2\ OH^- \rightarrow Cu(OH)_2^- + e \tag{1}$$

Recently, Fletcher et al. [20] have reported cyclic voltammetry measurements
on polycrystalline copper electrodes in 0.1 mol dm^{-3} LiOH. They concluded
that the first anodic process is dissolution of Cu(I). At somewhat higher poten-
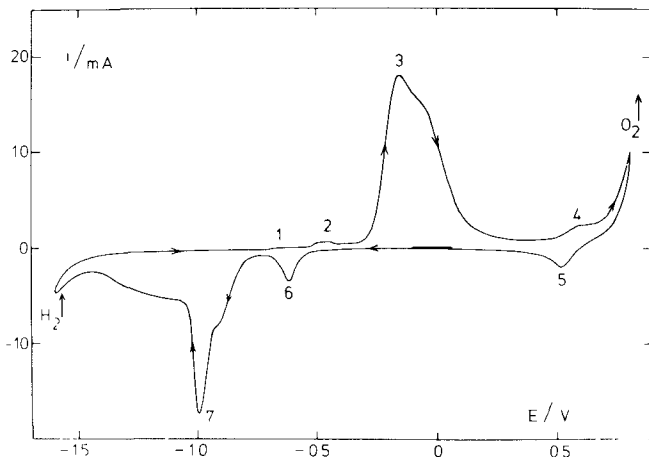
Fig. 1. Triangular sweep voltammogram for a copper electrode in 1 mol dm^{-3} NaOH after several oxidation and reduction cycles, $22°C$, $dE/dt = 90$ mV s^{-1}, E vs. "Argenthal" electrode (Ag/AgCl, KCl (3M)//, $E = 207$ mV vs NHE) Apparent surface area 0 28 cm^2.

tials, their voltammograms show a peak, which was attributed to the formation of a monolayer of Cu_2O, followed by a potential region where a thick Cu_2O layer is formed. Miller [8], on the other hand, concluded from experiments with rotating ring-disc electrodes that for Cu_2O no pre-film free dissolution could be detected. Therefore, the initial processes on copper anodes deserve further attention.

In this paper we report on combined electrochemical and ellipsometric measurements of carefully polished polycrystalline electrodes in NaOH solution. The ellipsometric technique was expected to give information on the possible formation of surface layers.

Our results indicate that the first stage in the anodising of copper electrodes (peak 1 in Fig. 1) is the electrosorption of oxygen species. This deposition occurs in two successive stages represented by two current peaks corresponding to different submonolayer states.

(II) EXPERIMENTAL

The working electrodes were copper discs (dia. 6 mm, thickness 4—5 mm) cut from a polycrystalline copper rod (Materials Research, 99.999% pure) and sealed into acrylic resin (Technovite 4071) in such a way that only the top surface of the metal was exposed to the solution. The electrodes were mounted on glass specimen holders, which were adjustable to allow proper alignment of the specimens to be studied by ellipsometry. The electrode surfaces were lightly rubbed with carborundum paper and polished with diamond pastes containing diamond particles as small as 0.25 μm, and then with alumina powders containing particles as small as 0.05 μm. Next the electrodes were, in some cases, chemically etched in 20% nitric acid. After polishing the electrodes were cleaned ultrasonically in twice-distilled water.

Before measurements were taken, the copper surfaces were cathodically

reduced at −1200 mV to remove any oxide films that might have been present. Sometimes it was necessary to activate the electrodes electrochemically to remove adsorbed impurities from the surface (see Section III.1.1).

An Ingold "Argenthal" electrode [Ag/AgCl, KCl (3M)]; E = 207 mV vs. NHE), separated from the main compartment, served as reference electrode. All potentials quoted in this paper are given with reference to this electrode. The wavelength of the ellipsometer light was 632.8 nm and the angle of incidence was 65 ± 0.5°. Further experimental details were the same as in ref. 21.

(III) RESULTS

(III.1) Cyclic voltammetry measurements

(III.1.1) Effect of potential sweep limit

Figure 2 shows a typical voltammogram recorded with a sweep rate of 20 mV s^{-1} and increasing sweep widths for the potential region of peak 1. Provided that the electrodes have been carefully cleaned, the general shape of the curves is the same for mechanically polished electrodes, electrodes etched in 20% nitric acid, and for electrodes that have been roughened by oxidation— reduction cycles over the potential region from −1.6 V to 0.8 V. With roughened electrodes the size of the voltammograms increased by a factor of about 4.
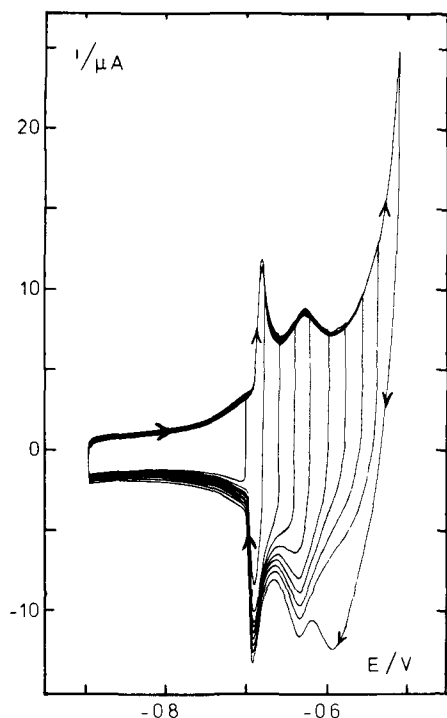
Fig. 2. Potentiodynamic charging curves for copper up to various potentials; 1 mol dm^{-3} NaOH, 22°C, dE/dt = 20 mV s^{-1}. Apparent surface area 0.28 cm^2.

Figure 3 shows that the voltammogram changes when the electrode is left in contact with the solution for several hours at a potential $E = -0.8$ V. Current densities are smaller, and the sharp peaks disappear. The original voltammogram can be found again after "electrochemical activation" of the electrode. The activation consists of applying some short oxidation pulses (0.1—0.2 s at $E = 1000$ mV), and of subsequently reducing the products formed at potentials where hydrogen evolution is just beginning.

The voltammograms in Fig. 2 clearly show two anodic peaks at potentials negative to the peak that corresponds to bulk formation of Cu_2O. The first is at —680 mV and has its cathodic counterpart at —690 mV. The second is at —630 mV and has its counterpart at —640 mV. The peak at —680 mV is very sharp and its half-width is estimated to be no more than 15 mV. Except in the case with the highest reversal potential, the current drops almost immediately to cathodic values after reversal of the potential sweep. It should be noted that the anodic curves almost coincide.

The charges under the anodic part of the curves are not markedly different from those in the corresponding cathodic parts. They are represented in Fig. 4. Comparison of the integrated charge-potential profile with the potentio-dynamic i—E curve shows that the Q—E line exhibits little structure in relation to that indicated differentially by the i—E curve itself.

Figure 5 gives a typical example of the changes in the ellipsometric parameters Δ and ψ as a function of the electrode potential during a triangular sweep. The plotted parameters $\delta\Delta$ and $\delta\psi$ are defined by $\delta\Delta = \bar{\Delta} - \Delta$ and $\delta\psi = \bar{\psi} - \psi$, where $\bar{\Delta}$ and $\bar{\psi}$ represent the parameters for the bare copper substrate at
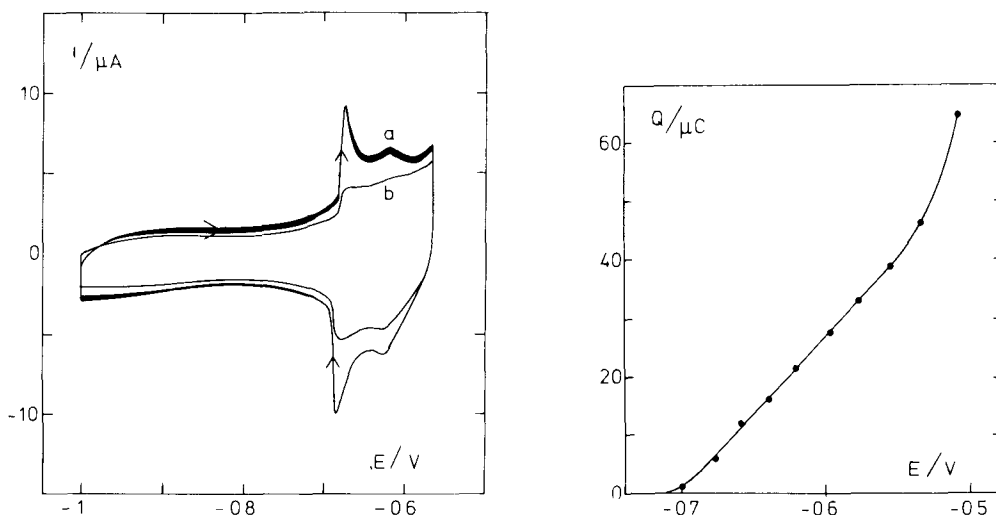
Fig. 3. Potentiodynamic charging curves for copper in 1 mol dm^{-3} NaOH, 22°C, dE/dt = 20 mV s^{-1}: (a) clean electrode surface; (b) electrode surface left in contact with the solution for about 2 h at a potential $E = -0.8$ V.

Fig. 4. Charges vs. the potential of scan reversal. Cu in 1 mol dm^{-3} NaOH, 22°C, dE/dt = 20 mV s^{-1}.
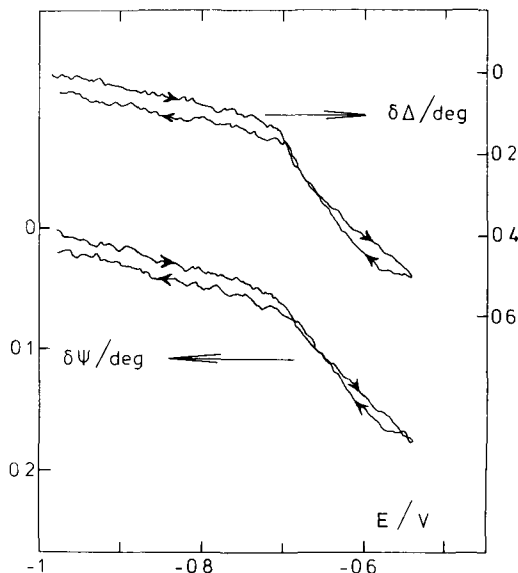
Fig. 5. Change in Δ and ψ during potential scanning up to -540 mV. Cu in 1 mol dm^{-3} NaOH, 22°C, $dE/dt = 20$ mV s^{-1}.

-1000 mV. The values of $\overline{\Delta}$ and $\overline{\psi}$ were measured for 15 different electrodes. From these we calculated the optical constants of the pure copper, which proved to be $n = 0.39 \pm 0.13$ and $k = 3.80 \pm 0.22$. We found that the ellipsometer light had no influence on the cyclic voltammograms. Figure 5 shows a slow increase in both $\delta\Delta$ and $\delta\psi$ in the region -1000 mV to -700 mV. At -700 mV there is a much sharper increase in $\delta\Delta$ and $\delta\psi$. There is a very little hysteresis between the positive and the negative sweep.

(III.1.2) Effect of sweep rate

Voltammograms were measured at sweep rates s varying from 10 mV s^{-1} to 2 V s^{-1}. For the two anodic and the two cathodic peaks in the voltammograms, plots of ln i_p vs. ln s give straight lines with slopes between 0.90 and 0.94. The peak potentials hardly shift (10—20 mV) with increasing sweep rate. In Fig. 6 the anodic charges Q_a are plotted for voltammograms measured at different sweep rates. The potential of sweep reversal was -580 mV. Maximum values of $\delta\Delta$ during a potential sweep are plotted in the same figure.

(III.2) Cyclic voltammetry with potential sweep arrest at the upper potential

Figure 7 shows voltammograms at a sweep rate of 20 mV s^{-1}, where the sweep was arrested at various potentials E_u of sweep reversal for 0, 15, 30 and 60 s. The charges under the cathodic current peaks indicate whether or not extra oxidation products have been formed during the sweep arrest. From Figs. 7a and 7b it is clear that during the first 15 s of waiting time a little more oxidation has taken place, because the cathodic currents are slightly higher. The curves
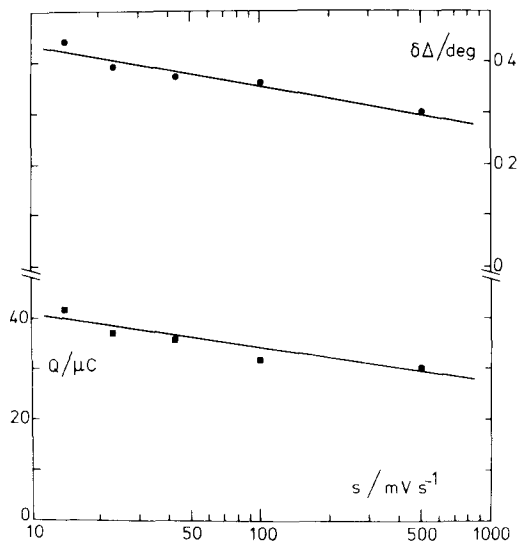
Fig. 6 Q_a and $\delta\Delta$ vs. sweep rate s

where $t = 30$ s coicide exactly with those where $t = 15$ s. Also in Fig. 7c the further oxidation can be seen to have been small. Here a very slight difference can be seen between the curve with a waiting time of 15 s and that with a waiting time of 30 s. In the voltammograms with an arrest potential of −540 mV the charge under the cathodic current keeps increasing considerably with waiting
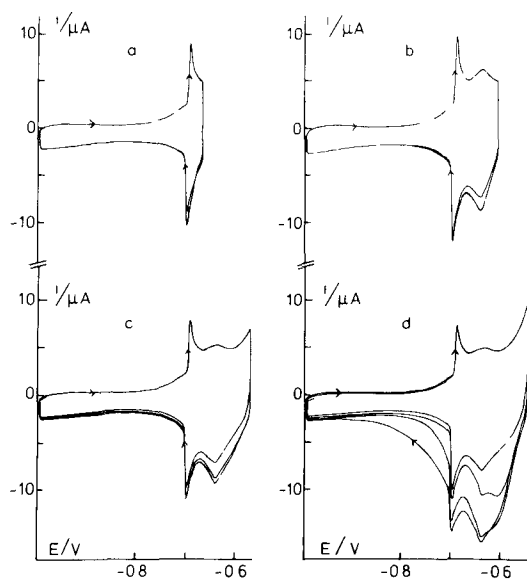
Fig. 7. Voltammograms with potential-sweep arrest of t seconds at the upper potential. Cu in 1 mol dm^{-3} NaOH, 22°C, $dE/dt = 20$ mV s^{-1}; (a, b, c) $t = 0$, 15 and 30 s; (d) $t = 0$, 15, 30 and 60 s. E_u = −660 mV (a); −600 mV (b); −560 mV (c); −540 mV (d).

time. Part of the reduction current is now shifted to potentials more negative than −700 mV. In this case the ellipsometric measurements also show a continuing increase in $\delta\Delta$ during the sweep arrest. The peak potentials of the cathodic waves do not shift with waiting time in any of the voltammograms in Fig. 7.

(III.3) Potential step measurements

Current responses to single potential step perturbations with starting potential −0.8 V and upper potential E_u in the region −700 mV to −500 mV are shown in Fig. 8. The potential step was followed by a negative potential sweep, with a sweep rate of 20 mV s^{-1}. The current–time curve contains information about the kinetics of the oxidation process. The charge under the cathodic reduction curve gives the amount of oxidation products, and the potentials of the cathodic current peaks give some indication of the character of the anodically formed species.
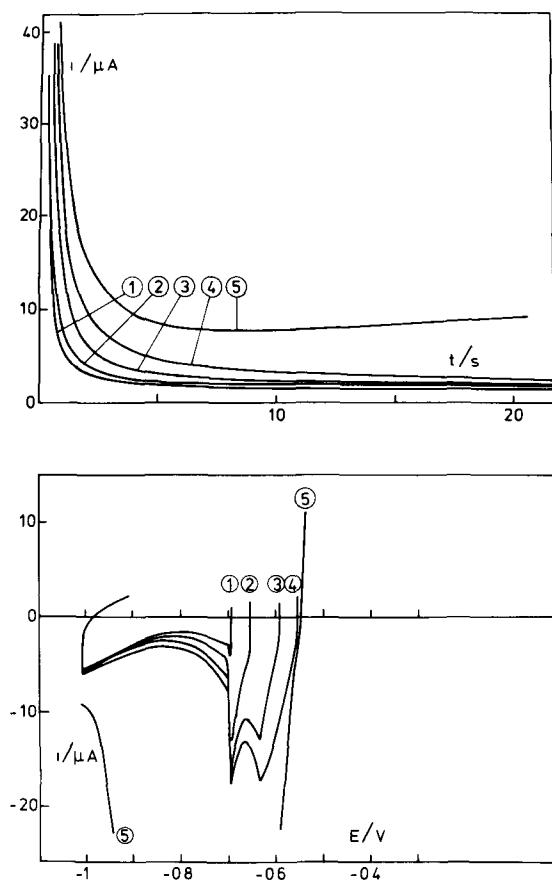
Fig. 8. Potential step measurements (starting potential −0.8 V) followed by potentiodynamic reduction (dE/dt = 20 mV s^{-1}). (1) E_u = −695 mV; (2) E_u = −655 mV; (3) E_u = −590 mV; (4) E_u = −555 mV; (5) E_u = −540 mV.

The current—time curves are all monotonically falling curves, with the exception of the curve at E_u = —540 mV where after about 10 s the current starts rising again. In the reduction curves it is seen that the amount of charge increases markedly between E_u = —555 mV and E_u = —540 mV.

(IV) DISCUSSION

The reversible Cu/Cu_2O potential at a pH = 14 is known to be —563 mV vs. the "Argenthal" reference electrode [22]. In Fig. 2 two anodic peaks are seen in the voltammogram at potentials lower than this reversible potential for bulk oxide formation. The ellipsometric curves in Fig. 5 show that there is a clear change at a potential of —700 mV, i.e. at the beginning of the first peak in the voltammogram. In this region no detectable surface roughening occurs; as from the first sweep the current—voltage curves remain the same, as do the ellipsometric parameters $\bar{\Delta}$ and $\bar{\psi}$. It is thus clear that the anodic peaks in Fig. 2 represent electrosorption of oxygen species and that the cathodic peaks represent the corresponding desorption process.

With potential sweeps up to —550 mV with a sweep rate of 20 mV s^{-1}, the deposition process is accompanied by an amount of charge of 40 μC. If for our electrodes the roughness factor is taken as 1 and an equal distribution of the three lowest index planes is assumed, then a complete monolayer of Cu(I) atoms corresponds to 70 μC.

The voltammograms in Fig. 2 show that electrosorption of oxygen species occurs in two successive stages each represented by a peak corresponding to a different submonolayer state, with a different adsorption energy. The problem here is whether or not the multiple states of oxygen chemisorption arise simply because of *a priori* heterogeneity of the surface, e.g. exposure of various crystal planes in which the adsorption sites have different energies. The fact that the current peak at —680 mV is very sharp indicates the existence of areas on the electrode which have only one type of adsorption site, with attractive lateral interactions between the adsorbed species [29,30]. For example, *a priori* heterogeneity has been found in the underpotential deposition of metal atoms on foreign metal substrates [23] and, very recently, in hydrogen chemisorption on platinum electrodes [24]. Gas phase studies have shown that oxygen chemisorption on copper single crystals is a very plane-specific reaction, and that the Cu(110) surface is much more reactive to oxygen than the (100) surface, which in turn is more reactive than the (111) surface [25—28]. However, the existence of *a priori* heterogeneity can be proved only by investigating this electrochemical reaction at carefully prepared copper single crystal surfaces.

Figure 3 shows that when the electrode is left in contact with the electrolyte for a long time, the electrode becomes contaminated. This means that a number of adsorption sites are blocked and are no longer active in the chemisorption of oxygen species. Apparently these adsorbed impurities can be oxidised anodically, and the reaction products can be removed at potentials where hydrogen evolution is just beginning.

The scan arrest measurements do not show any shift of the cathodic current peak, so an "ageing" process such as that reported for oxygen chemisorption on platinum and gold electrodes [31—33] was not found.

At the highest potential (Fig. 7d) the oxidation becomes more and more irreversible in the sense that a more cathodic potential is required to reduce the oxide film. At potentials lower than -560 mV, the oxidation—reduction behaviour of copper is rather reversible, compared to noble metal electrodes where hysteresis occurs between oxide formation and reduction of the surface oxide film [34—35].

From the identical dependence of Q_a and $\delta\Delta$ on the sweep rate s (Fig. 6) we conclude that $\delta\Delta$ is proportional to the charge Q_a and that there is no evidence for dissolution of copper species. This is in contrast with measurements on silver electrodes in NaOH [21], where considerable dissolution of silver species was shown to occur.

Current—time curves in Fig. 8 are monotonically falling curves. This means that there is random electrodeposition, because otherwise a peak, characteristic for a nucleation and growth process, would have been found in the i—t profile. The same conclusion follows from the voltammograms in Fig. 2 where, upon sweep reversal, there is never a continuing increase of current. The initial part of the i-t curve at -500 mV is not essentially different from the initial parts of the other curves. This means that at potentials for formation of bulk Cu_2O a surface film is first formed, and this is followed by in-depth oxidation.

(V) CONCLUSION

The first stage in the anodic oxidation of polycrystalline copper electrodes in NaOH solutions is the electrosorption of oxygen species. The process occurs in two successive stages, represented by two current peaks, corresponding to different submonolayer states.

ACKNOWLEDGMENTS

REFERENCES

1 E. Müller, Z. Elektrochem., 13 (1907) 133.
2 W. Feitknecht and H.W. Lenel, Helv. Chim. Acta, 27 (1944) 775.
3 A. Hickling and D. Taylor, Trans. Faraday Soc., 44 (1948) 262.
4 J.S. Halliday, Trans. Faraday Soc., 50 (1954) 171.
5 R.W. Ohse, Z. Phys. Chem. N.F., 21 (1959) 406.
6 M.J. Dignam and D.B. Gibbs, Can. J. Chem., 48 (1970) 1242.
7 H.P. Leckie, J. Electrochem. Soc., 117 (1970) 1478.
8 B. Miller, J. Electrochem. Soc., 116 (1969) 1675.
9 N.A. Hampson, J.B. Lee and K.J. MacDonald, J. Electroanal. Chem., 32 (1971) 165.
10 P.L. Bonora, G.P. Ponzano and M. Bassoli, Ann. Chim., 62 (1972) 636.
11 J. Ambrose, R.G. Barradas and D.W. Shoesmith, J. Electroanal. Chem., 47 (1973) 47.
12 J. Ambrose, R.G. Barradas and D.W. Shoesmith, J. Electroanal. Chem., 47 (1973) 65.
13 D.D. Macdonald, J. Electrochem. Soc., 121 (1974) 651.
14 D.W. Shoesmith, T.E. Rummery, D. Owen and W. Lee, J. Electrochem. Soc., 123 (1976) 790.
15 D.W. Shoesmith, T.E. Rummery, D. Owen and W. Lee, Electrochim. Acta, 22 (1977) 1403.
16 D.W. Shoesmith and W. Lee, Electrochim. Acta, 22 (1977) 1411.
17 V.P. Severdenko, V.A. Labunov, E.M. Kosarevitsh, L.V. Kogietov and V.M. Parkum, Thin Solid Films, 41 (1977) 243.

18 V. Ashworth and D. Fairhurst. J. Electrochem. Soc., 124 (1977) 506.

19 A.M. Castro Luna de Medina, S.L. Marchiano and A.J. Arvía, J. App. Electrochem., 8 (1978) 121.

20 S. Fletcher, R.G. Barradas and J.D. Porter, J. Electrochem. Soc., 125 (1978) 1960.

21 J.M.M. Droog, P.T. Alderliesten and G.A. Bootsma, J. Electroanal. Chem., 99 (1979) 173.

22 N. de Zoubov, C. Vanleugenhaghe and M. Pourbaix in M. Pourbaix (Ed.), Atlas of Electrochemical Equilibria in Aqueous Solutions, Pergamon Press, London, 1966, p. 384.

23 D M. Kolb in H. Gerischer and C.W. Tobias (Eds.), Advances in Electrochemistry and Electrochemical Engineering, Vol. 11, Wiley, New York, 1978, Ch. 2.

24 K. Yamamoto, D.M. Kolb, R. Kotz and G. Lehmpfuhl, J. Electroanal. Chem., 96 (1979) 233.

25 F.H.P.M. Habraken, E.Ph. Kieffer and G.A. Bootsma, Surf. Sci., 83 (1979) 45.

26 F.H.P.M. Habraken and G.A. Bootsma, Surf. Sci., 87 (1979) 333.

27 F.H.P.M. Habraken, G.A. Bootsma, P. Hofmann, S. Hachicha and A M. Bradshaw, Surf. Sci , 88 (1979) 285.

28 F.H.P.M. Habraken, C.M.A.M. Mesters and G.A. Bootsma, Surf. Sci., to be published.

29 E. Gileadi and B.E. Conway in B.E. Conway and J.O'M. Bockris (Eds.), Modern Aspect of Electrochemistry, Vol. 3, Butterworths, London, 1964, Ch. 5.

30 A Sadkowski, J. Electroanal. Chem., 97 (1979) 283.

31 H Angerstein-Kozlowska, B.E. Conway and W B.A. Sharp, J. Electroanal Chem., 43 (1973) 9.

32 N R. De Tacconi, A.J. Calandra and A.J. Arvía, J Electroanal. Chem., 51 (1974) 25.

33 C M. Ferro, A J. Calandra and A.J. Arvía, J. Electroanal. Chem., 59 (1975) 239.

34 R. Woods in A.J. Bard (Ed.) Electroanalytical Chemistry, Vol. 9, Marcel Dekker, New York, 1976

35 G. Bélanger and A.K. Vijh in A K. Vijh (Ed) Oxides and Oxide Films, Vol. 5, Marcel Dekker, New York, 1977, Ch. 1.